

Article type: Full Article

Preclinical evaluation of porcine colon resection using hollow core negative curvature fibre delivered ultrafast laser pulses

Syam M.P.C. Mohanan¹, Rainer J. Beck¹, Nicholas P. West², Michael Shires², Sarah L. Perry², David G. Jayne², Duncan P. Hand¹, Jonathan D. Shephard¹

¹ Institute of Photonics and Quantum Sciences, Heriot-Watt University, Edinburgh, EH14 4AS, UK

² Leeds Institute of Medical Research at St. James's, University of Leeds, Leeds, LS9 7TF, UK

*Correspondence: sp29@hw.ac.uk

KEYWORDS: ((Ultrafast laser surgery, porcine colon, plasma mediated ablation, Negative curvature fibre, Thermal necrosis))

Abstract text. 12 point, double-spaced. Maximum length 200 words.

Ultrashort pulse lasers offer great promise for tissue resection with exceptional precision and minimal thermal damage. Surgery in the bowel requires high precision and minimal necrotic tissue to avoid severe complications such as perforation. The deployment of ultrashort lasers in minimally invasive or endoscopic procedures has been hindered by the lack of suitable optical fibres for high peak powers. However, recent developments of hollow core microstructured fibres provides potential for delivery of such pulses throughout the body. In this paper analysis of laser ablation via a scanning galvanometer on a porcine colon tissue model is presented. A thermally damaged region ($<85\ \mu\text{m}$) and fine depth control of ablation using the pulse energies 46 and 33 μJ are demonstrated. It is further demonstrated that such pulses suitable for precision porcine colon resection can be flexibly delivered via a hollow core negative curvature fibre (HC-NCF) and again ablation depth can be controlled with a thermally damaged region $< 85\ \mu\text{m}$. Ablation volumes are comparable to that of early stage lesions in the inner lining of the colon. This study concludes that the combination of

This article has been accepted for publication and undergone full peer review but has not been through the copyediting, typesetting, pagination and proofreading process, which may lead to differences between this version and the [Version of Record](#). Please cite this article as [doi: 10.1002/jbio.201900055](https://doi.org/10.1002/jbio.201900055)

ultrashort pulses and flexible fibre delivery via HC-NCF present a viable route to new minimally invasive surgical procedures.

1 INTRODUCTION

Since 1960, lasers have been extensively used in the medical application areas such as laser therapy [1-3] , laser surgery [4-6] , and laser diagnosis [7-9] . Over the last few decades, picosecond (ps) and femtosecond (fs) lasers have been deployed in laser surgery research related to soft [10-13] and hard [14-15] tissue ablation. These lasers have the ability to offer precise and rapid resection with minimal thermal and mechanical damage to the adjacent tissue in the surgical zone [16]. In contrast, the continuous wave laser, long-pulsed laser, and electrocautery based conventional surgery techniques are all prone to significant thermal damage [17-18]. The light from a conventional long pulsed laser is absorbed by the superficial tissue layer. Thus, the absorbed laser pulses lead to an effective thermal resection with thermal damage to the adjacent healthy tissue in the order of 300 microns [17]. This surgical modality is not a good choice for intestinal surgery because the colonic polypectomy or local excision demands high precision and minimal thermal damage due to the thin walled structure of the bowel. Bowel perforation, as result of endoscopic or laparoscopic surgery, is considered one of the most severe post-surgery complications [19-20]. Precise control of the width of tissue damage and depth of resection are of paramount importance to avoid bowel perforation.

The application of plasma induced effects in surgery was initially reported by Krasnov [21] and Aron-Rosa et al. [22] . The use of long pulsed lasers for the endoscopic treatment of gastric tumours are also reported during the same period [23-24]. The surgeons have performed experimental studies on the bowel tissue of animals to assess the thermal damage mechanism and haemostasis ability of long-pulsed laser scalpels and electrocautery tools [25]. They concluded that the thermal necrosis induced by these surgical modalities are similar in

nature. It is unsurprising therefore that established electrocautery based surgical procedures have continued as the standard method for colonic polypectomy and colon tumour resection because the long pulsed laser has no significant improvement in reducing thermal damage. Until recently, the implementation of ultrashort pulsed lasers in colon surgery or colonoscopy was impossible because of the lack of a suitable delivery optical fibre. Although silica is an ideal bio-inert material for clinical use, the low damage threshold and high nonlinearity prevents conventional solid core silica fibres from carrying these high energy laser pulses. Recently, the delivery of high peak power 1030 (up to 92 μJ pulse energy with a core diameter of $\sim 38\text{ }\mu\text{m}$) and 515 nm picosecond lasers via 8 cell silica hollow core negative curvature fibres (HC-NCF) has been demonstrated [26-27]. These fibres guide via the anti-resonant reflecting optical waveguide (ARROW) mechanism [28]. The role of hollow core negative curvature fibre (HC-NCF) in industrial and medical applications has also been recently reported [29]. The experiments reported here were designed to investigate the pre-clinical evaluation of a ps laser in colon tissue resection. Preliminary studies on colon tissue resection based on ultrafast laser pulses delivered via a galvanometer have been reported recently [30-31]. Researchers have been used multicore [32] and graded index multimode [33] fibres for the delivery of ultrashort pulse to demonstrate the laser ablation. Prior work has established pig tissue as an efficient medical model for several studies related to human diseases [34] and is consequently applied in porcine vocal fold tissue resection using 1.5 ps laser pulses delivered through kagome lattice hollow core photonic crystal fibre for microsurgery [35]. The microsurgery laser ablation on the vocal fold tissue has a depth and width of ablation of around 43 and 40 μm respectively at a pulse energy of 1.2 μJ .

In contrast to previous work in fibre delivered ultrashort pulses for microsurgery of tissue [35-36] the work reported here focusses on using longer, 6 ps, pulses for larger, mm scale,

ablation of tissue. These pulses are delivered using a HC-NCF which has favourable performance in terms of minimising nonlinear effects and bend losses. Pulse energies of up to 28 μJ were successfully delivered to the porcine colon surface without any damage to the fibre. Using such pulses with a scanning modality the ablated zone width is approximately 25 times that reported in the vocal fold microsurgery work described above. Additionally, the process developed here is more relevant to the size of early stage colonic lesions and polyps compared to previous microsurgery techniques. The aim was to be able to resect such lesions and polyps from the inner lining tissue of the colon tissue by adopting a scanning strategy tailored to the size of the lesion.

According to Cancer Research UK data, the second highest number of cancer deaths in the United Kingdom occurs due to bowel cancer [37]. The early diagnosis and treatment of colon cancer its precursor, adenomatous polyps, are important to reduce the rate of mortality. The stages of colon cancer are determined by the extent of spread through the layers of the bowel wall and whether the localized tumour has spread to lymph nodes or distant organs. The surgical removal of colon polyps or cancers based on conventional techniques may lead to two of the most important post-surgery complications, bleeding and perforation [38]. In this paper we demonstrate the relevance of ultrafast laser in colon tissue resection for minimal perforation or thermal damage. Figure 1 shows a schematic of the colon structure. The innermost layer of the colon is known as the mucosa, which consists of epithelial cells arranged in crypts, connective tissues and a thin smooth muscle layer at the base. The submucosa consists of connective tissue containing blood vessels, lymphatic vessels and nerves. The muscularis propria is the main muscle layer of the bowel and has an inner circular and an outer longitudinal layer. The outermost adventitia or sub serosa is composed of connective tissue with the larger blood and lymphatic vessels along with lymph nodes. Our

objective is to resect colonic polyps or cancer cells in the mucosa and submucosa, i.e. the area in between the two red circles in Figure 1.

The high peak intensity ($>10^{11}$ W/cm²) of the picosecond laser at the tissue surface means that the light is strongly absorbed via nonlinear processes, generating a plasma. Once initiated the plasma absorbs the rest of the laser energy and efficaciously couples the energy to the tissue to create a non-thermal surgical effect [39] and hence tissue resection with precise crater size, shape, depth and minimal thermal damage. This study investigates the depth of this tissue resection and width of thermal necrosis as a function of pulse energy and laser fluence with constant pulse repetition rate (PRR) and pulse overlap in an ex-vivo porcine model using a scanning galvanometer and fibre optic system. The histology and three dimensional (3D) optical profilometric results of the surgical zone are used to analyze the effect of laser parameters in tissue ablation.

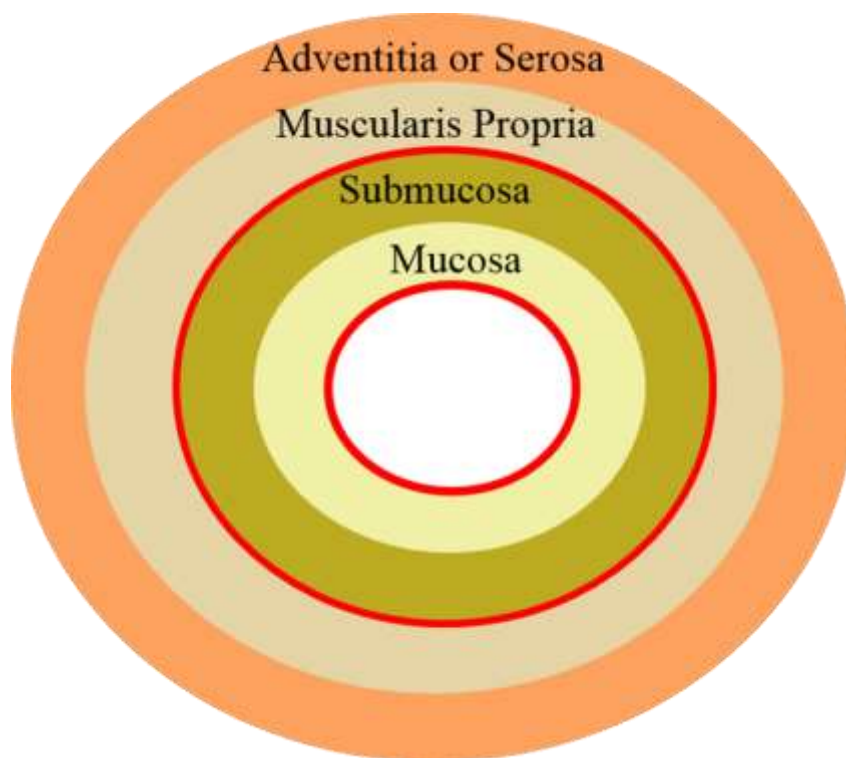


Figure 1 Schematic representation of colon tissue layers.

2 MATERIALS AND METHODS

2.1 Experimental systems for fibre delivered and direct laser resection of porcine colon

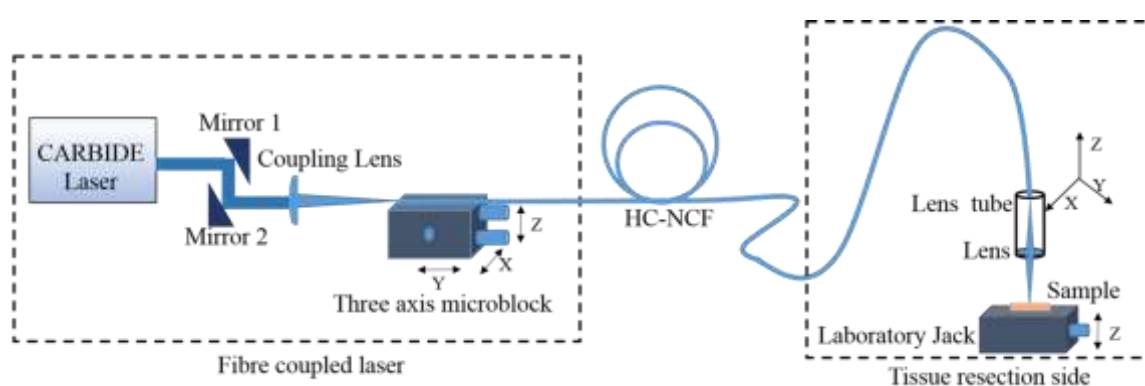


Figure 2 Schematic of the laser system for fibre delivered pulses for tissue resection

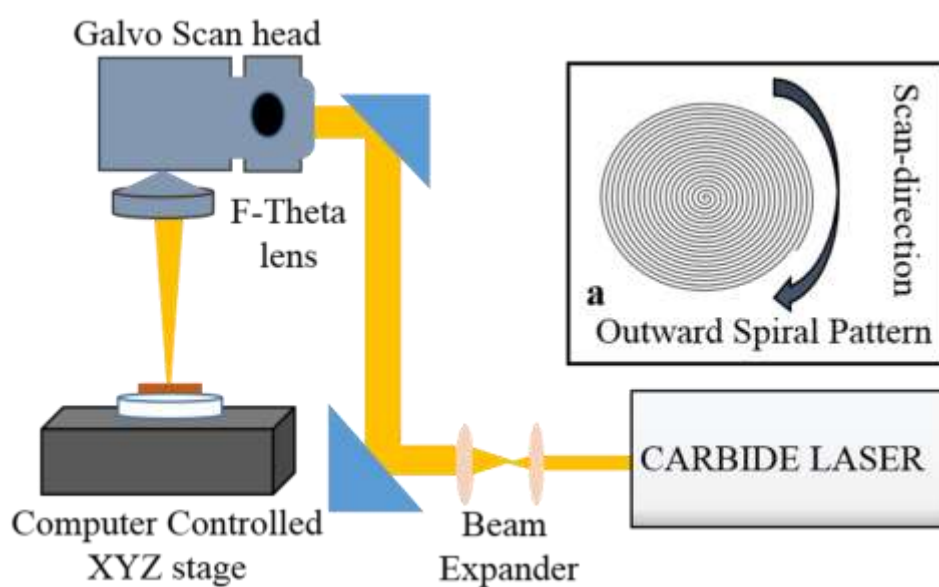


Figure 3 Schematic of the laser system for direct laser resection of tissue a) Schematic of the spiral scan pattern at the colon tissue surface during picosecond laser ablation

Figure 2 shows the experimental system for the tissue resection using fibre delivered ultrashort pulses (USPs). An industrial laser (Light Conversion CARBIDE) with a central wavelength of 1028 ± 5 nm, a range of base repetition rates from 60 kHz to 1 MHz and a tunable pulse width ranging from 232 fs to 10 ps was used. A maximum average power of 5 W and a base repetition rate of 60 kHz was used for the application. The experiment was conducted using a 6 ps pulse width to avoid the nonlinear effects in the fibre observed when delivering similar pulse energies in the femtosecond regime. The axial displacement of the tissue was achieved by a manual lab jack connected with a dial gauge to find accurate focus. The fibre end probe (consisting of focusing optics) is attached to the movable arm of the multi-axis robotic device (AxiDraw V3). The fibre end probe consists of a ~77 mm long slotted lens tube, a fibre connector and its adaptor, retaining rings and a plano convex lens with 20 mm focal length. The cleaved output end of the 1.5 meter long HC-NCF was connected to the fibre connector and was attached to the lens tube using an adaptor. The focussing optics had minimal effect on the pulse energy/fluence transmitted through the fibre. The laser pulse energy without the focusing optics was ~29 μ J and after the 20 mm lens the pulse energy was reduced to ~28 μ J. During the scanning process, there was no relative movement of the focussing optics and fibre, which ensured uniformity of the laser pulse energy/fluence distribution on tissue surface. The experimental system used to investigate direct laser ablation of colon tissue using the same laser is shown in Figure 3. This uses a galvanometer scanhead plus F-theta lens of focal length 100 mm, and Figure 3a shows the spiral scan pattern that is employed in this case.

2.2 High peak power pulse delivery through HC-NCF

When transmitting USPs through the solid core fibres, pulse distortions occur as a consequence of the nonlinear effects generated in the fibre such as self-phase modulation and self-focusing [40-41]. Conversely the proposed HC-NCF guides the laser light through the air core based on anti-resonant reflecting optical waveguide (ARROW) technique [28]. The hollow core minimizes the nonlinear effects in the fibre due to high peak power pulse delivery, and provides a much higher damage threshold than a solid core fibre. However, the optimization of the power delivered through the HC-NCF is challenging due to the low numerical aperture (0.044) and small core diameter of the fibre ($\sim 21 \mu\text{m}$). If not correctly aligned, the high peak power pulses induce damage at the light coupling end face of the fibre.

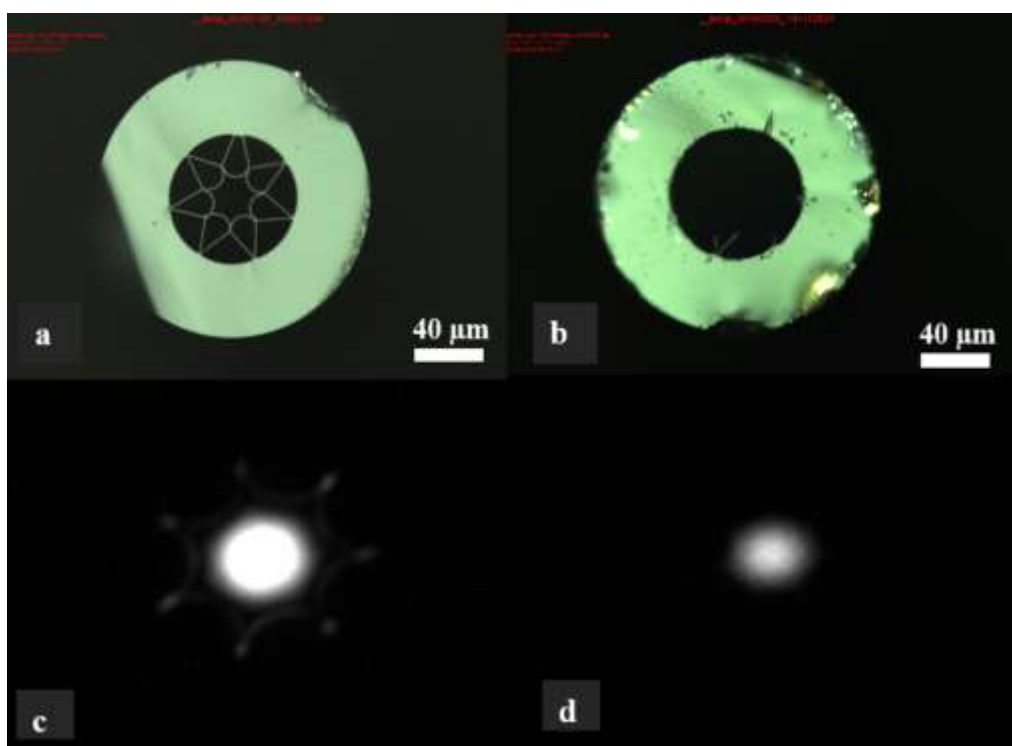


Figure 4 Seven cell NC-HCF fibre (a) cleaved laser launching surface (b) damaged surface (c) image of light confined in a single mode at the end face of HC-NCF (20x zoomed image) (d) single mode beam at the focus of 20 mm focal length lens (20x zoomed image) placed after the HC-NCF.

In order to achieve a high coupling efficiency it is necessary to have a high quality cleaved fibre end, whilst matching the mode field diameter (MFD) and numerical aperture (NA) of the input beam with that of the fibre. The Figure 4a shows the cleaved end face of the HC-NCF at

the laser coupling side. Figure 4c shows the light confinement of the single mode beam in the core of the fibre and Figure 4d shows the single mode beam at the focus. The minimum bending radius used for this experiment was 20 mm. It has been previously reported that the minimum bend radius of the HC-NCF before resonant bend loss occurs is 7.5 mm [42]. The minimum bending radius of a typical colonoscope is around 25 mm [43] determined using bend sensors in a standard colonoscopy training model. The power output and the single mode profile at 20 mm bending radius of the HC-NCF is presented in figure 4. At this bend radius laser power transmission is not affected, which is evident in figure 5.

We repeatedly achieved a coupling efficiency of ~70% without damage to the fibre. Figure 5 shows the coupling efficiency plot of the 7cell HC-NCF and shows a coupling efficiency of 70 % from the laser to the fibre up to the input pulse energy of approximately 42 μJ and peak power of 7 MW. At approximately 50 μJ the onset of damage to the input facet of the fibre occurs and is observed by the fact that the output energy no longer increases with increasing input energy. At an input pulse energy of 71 μJ (peak power of 11.8 MW) total destruction of the core and cladding structure occurs shown in Figure 4b and the fibre is no longer able to guide the laser pulses. Therefore, for these experiments the practical input energy was limited to less than 50 μJ . Power stability experiments for the HC-NCF were carried out at maximum output power, without any damage to fibre, for up to 2 hours. During this period output power varied between 1.747 and 1.742 W.

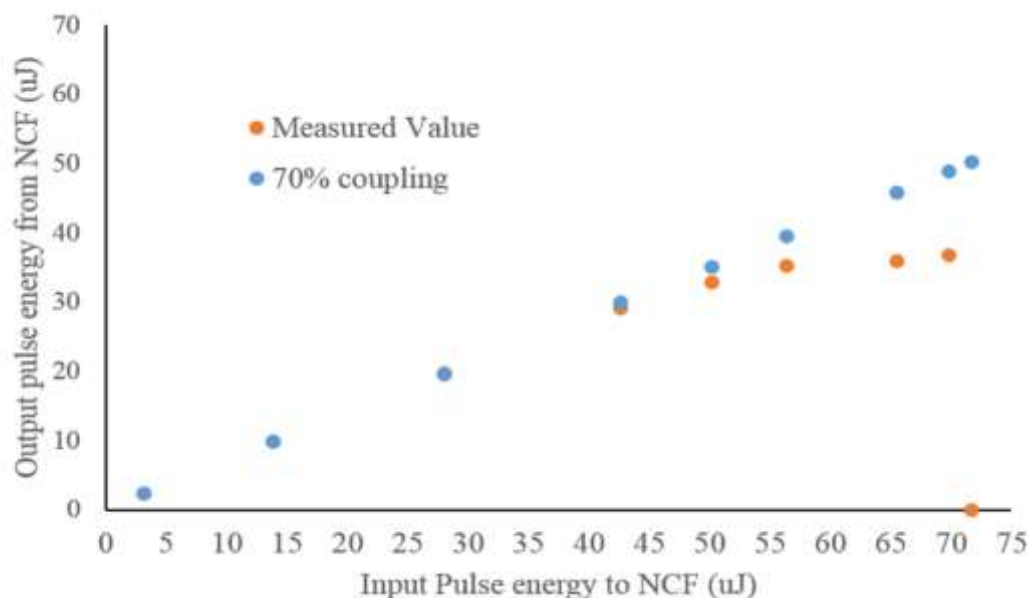


Figure 5 Coupling efficiency plot of 7 cell HC-NCF

An autocorrelator was used to measure the pulse length of the laser beam directly output from the laser, and after it has been delivered through 1.5 m of the HC-NCF, to assess fibre dispersion. The results are shown in Figure 6, demonstrating that any dispersion effect is minimal in this length of fibre for a $\sim 29 \mu\text{J}$ pulse. The actual pulse width is 0.65 times the width of autocorrelation traces [44]. Meanwhile, the spectral content of the laser and the fibre delivered beams is shown in Figure 7; the minimal difference demonstrates that nonlinear effects such as soliton formation, self-focusing or Raman scattering do not occur in this fibre [45-47]. However, a slight shift in the centre wavelength is noted, likely due to the non-uniform attenuation of the HC-NCF at the wavelength of interest (measured).

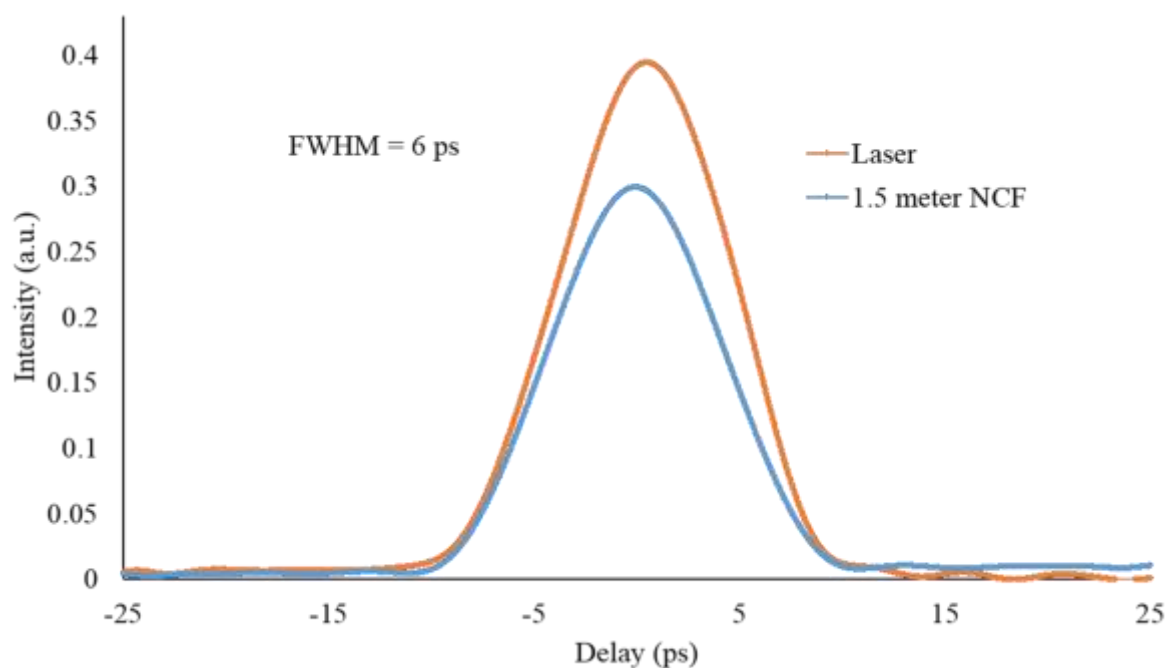


Figure 6 Autocorrelation traces of picosecond laser beam (FWHM = 6ps) with an input pulse energy of $\sim 42 \mu\text{J}$ corresponding to $\sim 29 \mu\text{J}$ delivered from the output of the HC-NCF (Blue line) showing no significant pulse broadening.

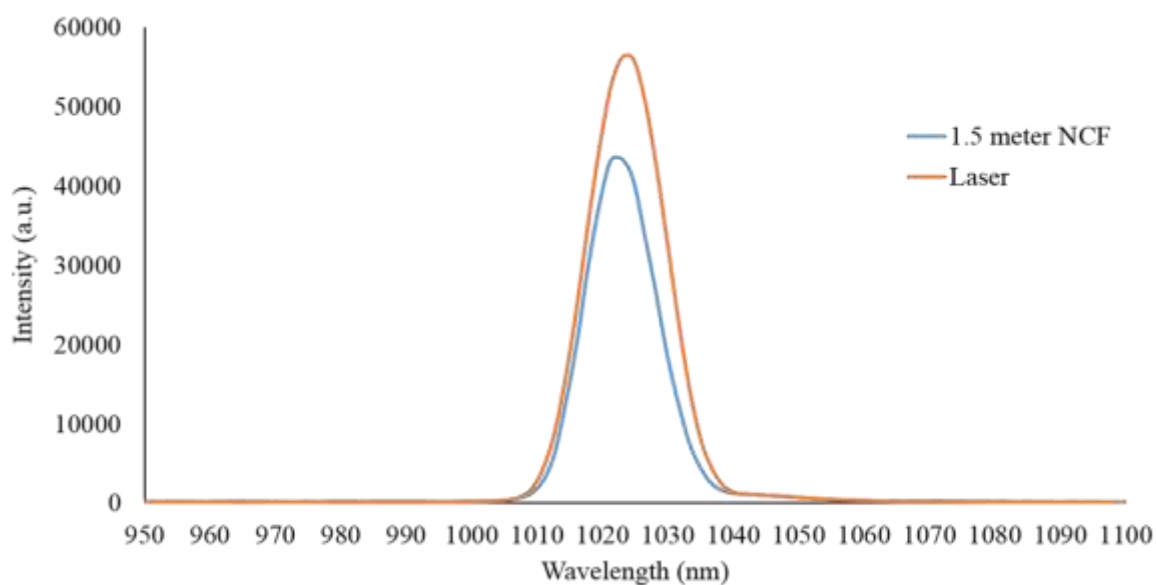


Figure 7 Optical spectra of laser beam of 6 ps pulse width and $42 \mu\text{J}$ pulse energy. 1.5 meter long HC-NCF delivered beam with 6 ps pulse width and $\sim 29 \mu\text{J}$ pulse energy (blue line).

2.3 Sample preparation

For the experimental work pig colon tissue samples were extracted from mature pigs immediately after postmortem and stored in phosphate buffered saline (PBS) solution. Laser processing was carried out no longer than 48 hours of postmortem to ensure that the tissue was still viable and subsequent histological observations would be clinically relevant. Post laser processing, one set of samples fixed in 4% aqueous solution of formaldehyde were embedded into paraffin wax by standard procedures. Sections cut at 4 microns onto glass microscope slides and stained with Haemotoxylin and eosin were used for histological analysis in order to measure the dimensions of the laser excision and width of coagulated necrosis. Another set of samples were used for microscopic studies after glutaraldehyde fixation. All experimental procedures were conducted according to the protocols approved by the Heriot Watt University ethics committee on biological tissue handling.

2.4 Experimental methodology

For direct laser resection of colon tissue via the galvanometer, a spiral scan pattern of 2 mm diameter on the tissue surface was used to ablate tissue with approximately 90% pulse overlap in the laser scanning and line separation direction. A laser PRR of 10 kHz was used, with pulse energies of both 46 and 33 μJ , and corresponding fluences of 18, 13 J/cm^2 respectively. These pulse energies were selected because of the fluence generated for this ablation was close to the fluence used for the fibre based colon resection. These experiments were mainly focused on assessing the ablation depth and thermal damage according to the change in laser pulse energy and average laser fluence. The spot size was verified using a scanning slit beam profilometer (DataRay, Beam Map2). Using the f-theta lens the focussed spot diameter was measured as 18 μm . All laser fluences were calculated using Eq. (1) [48].

$$E_p / \pi \omega_0^2 \quad (1)$$

where E_p is the pulse energy and ω_0 is the radius of the spot size at the tissue surface.

In HC-NCF delivered laser pulse resection of colon, the fibre end probe was connected to the XYZ multi-axis robotic device controlled by a software package (Inkscape). For the HC-NCF delivered laser pulse ablation trials, a spiral scan pattern of 1 mm diameter was performed on the surface of the porcine colon. This experiment was carried out at 10 kHz PRR to achieve approximately 90% pulse overlap in laser line separation and scanning direction (to match that used in the galvanometer experiments). Using 10 kHz PRR, the multi axis robotic device can be moved at a speed that avoids unwanted vibrations. Using a higher PRR requires the device to be moved at higher speeds (to maintain the correct pulse separation) where significant vibration occurs. Three outward spiral patterns were performed on the tissue surface with laser fluence of approximately 21, 14 and 7 J/cm² respectively, providing similar conditions to the fibre delivered laser ablation trials.

For both the above experiments the focal position of the laser on the tissue surface was located first, before carrying out a scanning pattern, by using a series of single pass ablation lines whilst varying the separation between the tissue sample and the final focussing lens.

2.5 Profilometric characterization of tissue samples

An Alicona Infinite Focus profilometer is used to examine the depth profile and the three dimensional (3D) surface profile of surgical zone in the tissue sample [49].

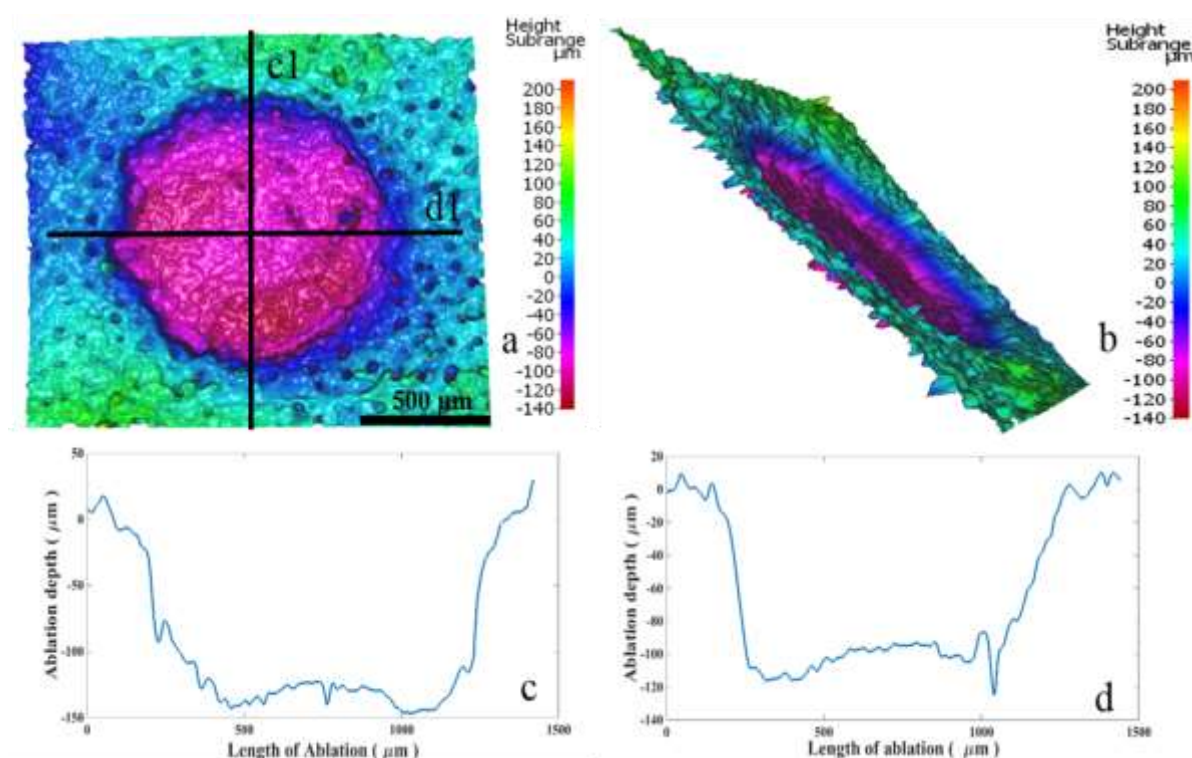


Figure 8 (a) and (b) Three-dimensional surface profile of the laser ablated zone, (c) and (d) orthogonal depth profiles of the same crater.

In Figure 8, 8a shows the 3D profile of the laser ablated zone created using the multi axis fibre scanning system with 7 J/cm^2 laser fluence, 90% pulse overlap in the 1 mm diameter spiral scan pattern. Figure 8c and 8d shows the orthogonal cross sections of the surgical zone and the depth profile measured through the centre of the cavity. The lines c1 and d1 through the centre of the crater represent the depth profiles 8c and 8d respectively. The average depth and standard deviation of the ablated zone was calculated by taking the mean value of the individual average depth and standard deviation of horizontal and vertical depth profiles.

3 RESULTS AND DISCUSSION

The histology images are helpful for identifying tissue damage and ablation depth after the laser resection of colon tissue. Such histology results are used in the literature to prove the efficiency of the laser ablation [50-52]. The ablation depth and width of thermal damage was analysed in relation to applied laser fluence. Figure 9 shows the histological pattern of laser

resected colon and the corresponding surface profile. The mucosal layer has been completely removed with a fluence of 13 J/cm^2 , while some of the submucosal area is also resected at the higher laser fluence (i.e. 18 J/cm^2), this is evident in the histology pattern. Figure 9 also shows the depth over the ablated region but it should be noted that some shrinkage of the profilometric samples occurred due to the glutaraldehyde fixation process. The white regions on the 3D images are missing data points which is a limitation of the device where it becomes difficult to receive reflected light signals from the sample areas which have a high slope angle or large height differences in the ablated region [49]. The average depths of 0.55 ± 0.18 and 0.44 ± 0.16 mm are achieved at 18 and 13 J/cm^2 laser fluence respectively. The standard deviation values depend on the uneven bottom surface of the crater. The depth of the laser ablated zones are indicated on the false colour scale bars. The change in ablation depth according to the laser pulse energy at 1 kHz of porcine colon has also been reported [30]. The results at 10 kHz and those previously reported at 1 kHz [30] confirm that the resection is controllable by adjusting the pulse energy and laser fluence with a minimal heat affected zone and hence demonstrates the viability for precision tissue resection. In 2016, Kaushik et. al. used a 100 μm thick porcine vocal fold tissue to investigate the ultrafast laser ablation characteristics. A laser with a pulse width of 1.5 ps, PRR of 303 kHz and wavelength of 776 nm was used to ablate the tissue with a maximum fluence of 7.8 J/cm^2 . The laser was transmitted through a kagome fibre optic probe, which was used to generate a lissajous pattern on the tissue surface at a frequency of approximately 1 kHz. However, no histology results are provided with this work so it is not possible to evaluate the impact on underlying tissue in a clinically relevant context and in particular assess the extent of the thermally damaged region [35]. Earlier research has shown a significantly larger width of thermal necrosis induced by conventional surgical devices such as electrocautery (456 μm) [53], harmonic scalpel (690 μm) and CO_2 laser (300 μm) [17]. In contrast, the histology results presented here, as shown

in Figure 9, demonstrate that a thermally damaged region of less than 85 μm and a maximum ablation rate of $1.07 \text{ mm}^3/\text{minute}$ are achievable with picosecond laser resection of porcine colon. The ablation rate has been calculated using the ratio of volume of the crater to the total time taken for ablation.

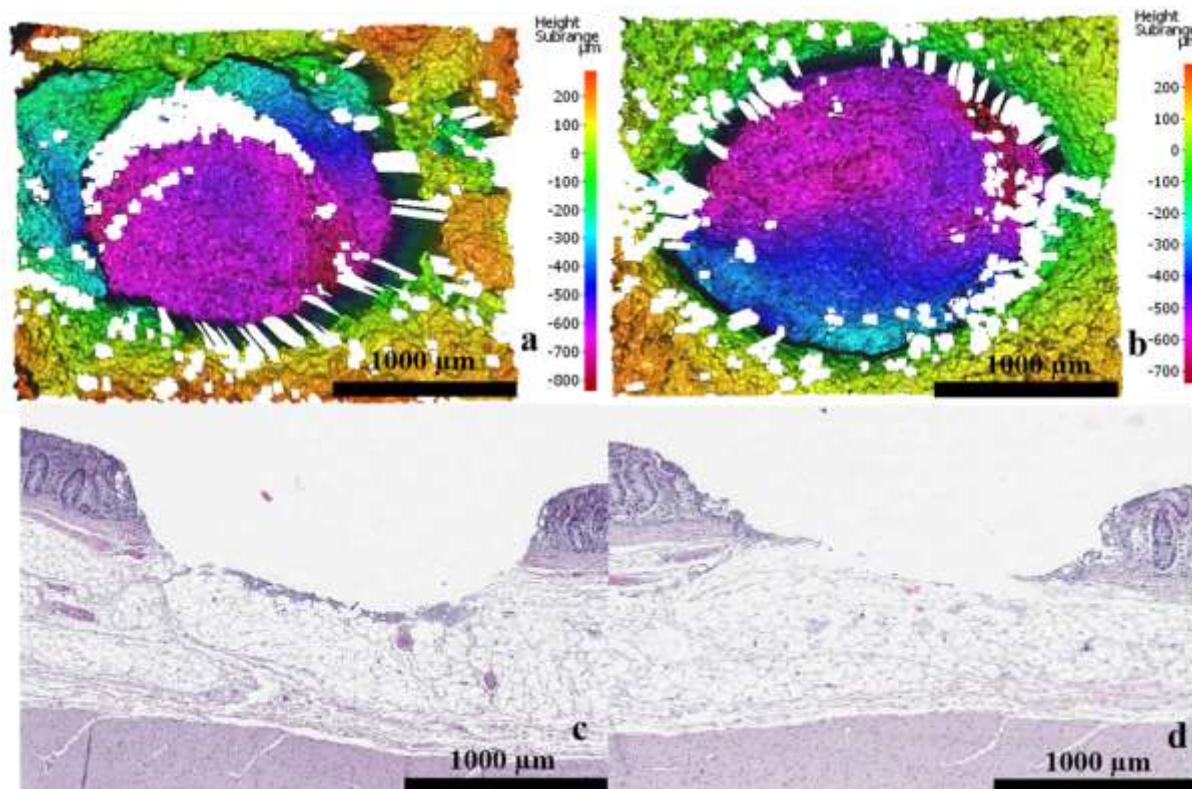


Figure 9 Haematoxylin and eosin (H&E) stained images and 3D profilometric images of laser ablated zones in different tissues using same laser parameters. The applied laser fluences are a & c) 18 J/cm^2 b & d) 13 J/cm^2

The results obtained from the galvanometer at 10 kHz (Figure 9) demonstrate that precise tissue ablation with limited necrosis to the surrounding tissue was possible using 6 ps pulses. However, in order to demonstrate a more surgically relevant modality demonstration of the tissue ablation was carried using the flexible HC-NCF to deliver pulses to tissue. During the laser ablation the fibre is manipulated via multi-axis robotic device to mimic a more practical arrangement that might be expected during a surgical procedure in an operating theatre. In a practical setup the laser would need to be located remotely from the patient on the operating

table. The fibre would then need to allow an arbitrary path to be followed around the theatre (likely to be a few metres from the laser to the endoscopic device) to avoid other pieces of equipment and not get in the way of the medical staff. The end of the fibre would be guided down the endoscope to the surgical site (in the colon for example). The fibre end-tip would then be manipulated or repeatedly scanned (rastered) over small distances (in the order of a few mm) during the surgical procedure. The experimental set-up (as shown in Figure 2) simulates this practical arrangement.

In the tissue resection experiments based on HC-NCF, the laser pulse energy measured after the focus lens in the fibre end probe was approximately 28 μJ . Using the spiral scanning pattern described above tissue resection was performed with the fibre delivered pulses. It is evident from the profilometric and histology analysis (Figure 10) of the laser ablated tissue, that the laser pulses transmitted through the HC-NCF are capable of precisely excising the biological tissue. The maximum ablation rate achieved for hollow core fibre based ablation was 0.17 $\text{mm}^3/\text{minute}$. The measured Rayleigh length for f-theta lens and fibre probe lens were ~ 300 and 135 μm respectively.

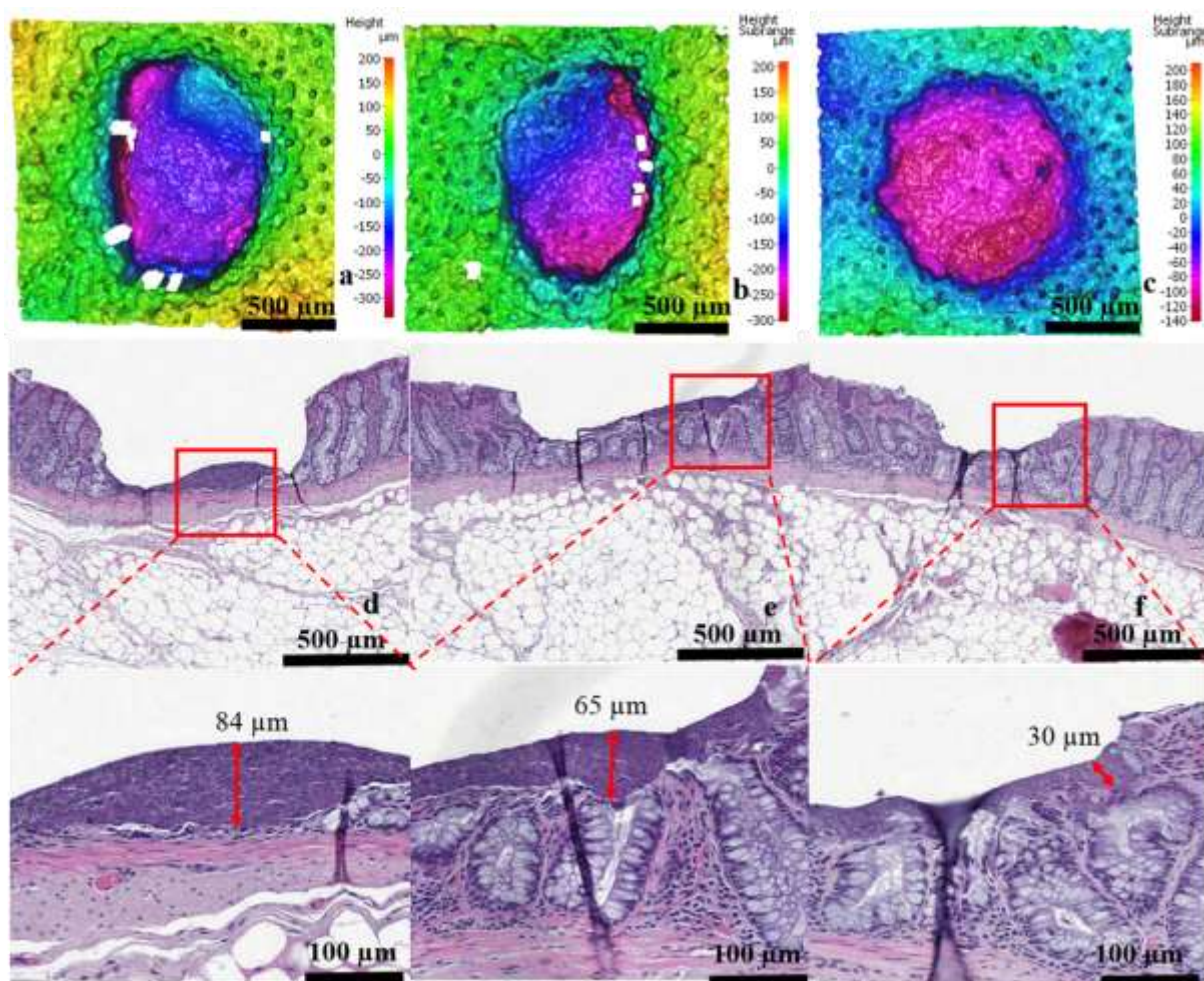


Figure 10 The 3D profilometric image of laser ablated area using HC-NCF delivered pulses on porcine colon samples and histology results of laser ablated area in different tissue sample with same laser parameters a) 21 J/cm^2 b) 14 J/cm^2 and c) 7 J/cm^2 laser fluences. The black line on the image is an artefact after the preparation of sample for histology. The expanded view of maximum thermal damage in each laser ablated tissue area is presented at the bottom of the figure.

The images in Figure 10 d, e and f are the H&E stained images of laser resected sections, which demonstrate that the maximum width of thermal necrosis was always less than 85 μm in this experiment. In colon tissue, thermal damage of approximately 84 μm , 65 μm and 30 μm are observed in laser fluence operations of 21 J/cm^2 , 14 J/cm^2 and 7 J/cm^2 respectively. The maximum width of thermal damage is marked in the corresponding zoomed images

(bottom three pictures of Figure 10). Nevertheless, the results presented, and in particular the ablation represented in Figure 10c and 10f, clearly demonstrate that it is possible to perform selective tissue surgery with negligible tissue damage (down to 30 μm) via the HC-NCF delivered pulses. The highest average ablation depth of $169 \pm 56 \mu\text{m}$ achieved at 21 J/cm^2 laser fluence and the lowest ablation depth of $87 \pm 28 \mu\text{m}$ achieved at 7 J/cm^2 laser fluence. The samples used for the 3D profilometry were geometrically distorted after the glutaraldehyde fixation, which is evident in figure 10 a and b. In the fibre delivered pulse ablation experiment, the removal of mucosal tissue was achieved. This depth of ablation is commensurate with the region in the colon where the early stage cancerous polyps develop [54-55]. The spiral pattern enabled an area similar in size to early stage lesions to be scanned whilst maintaining continuous scanning of laser pulses. Also, these fibre delivered results compare well with those produced using the galvanometer scheme. However, it should be noted that there is a difference in ablation depth, when using approximately similar fluences, between the direct (galvanometer) and fibre delivered laser experiments which is attributed to the difference in depth of focus. The galvanometer uses a 100 mm focal length lens whereas a 20 mm focal length lens is used for the fibre delivered laser ablation. In addition, it should be highlighted that the diameter of the raster scan pattern performed by galvanometer was twice that of the diameter of the raster scan pattern performed by the multiaxis fibre scanner. Nevertheless, the results presented here are a clear demonstration that this precision surgical modality could be transferable to the clinic using a delivery scheme based on HC-NCF.

One benefit of using the HC-NCF reported in this study, and using pulse widths of 6 ps, is the capability to mitigate the nonlinear effects when transmitting ultrashort pulses. In [36], the photonic bandgap fibre used exhibited nonlinear effects for delivery of 1.5 ps pulses. A maximum pulse energy of 2 μJ was achieved before damage of the fibre compared to stable

Accepted Article

delivery of 29 μJ for the HC-NCF. In [35] the delivery was limited to 1.4 μJ due to nonlinear effects of the fibre and ZnS lenses. Up to 4 μJ pulse energy could be transmitted through fibre and hence it was necessary to keep the focused spot size small (4.5 μm diameter) in order to generate high fluences required for ablation. Both [35] and [36] focus on microsurgery applications whereas the specific aim this study is resection of tissue at the mm^3 volume level. This is particularly relevant for the scale of early stage colonic tumours and hence it is clear from this study that using 6 ps pulses, delivered by a flexible HC-NCF, has potential for developing procedures that could successfully improve surgical treatment of such diseases.

4 CONCLUSION

In this study, it was demonstrated that ultrafast laser pulses are suitable for colon tissue ablation with a necrotic tissue width of $< 85 \mu\text{m}$. Average depths of 0.55 ± 0.18 and 0.44 ± 0.16 mm are achieved at 18 and 13 J/cm^2 laser fluence respectively. The HC-NCF can transmit 6 ps laser pulses with a maximum of 42 μJ pulse energy and delivered single mode laser beam of 29 μJ pulse energy without any change in 70% coupling efficiency, spectral quality and temporal quality of the pulse. The suitability of fibre delivered ultrafast laser beam in tissue surgery was established with a maximum average depth of $169 \pm 56 \mu\text{m}$ achieved at 21 J/cm^2 laser fluence and a minimum average depth of $87 \pm 28 \mu\text{m}$ achieved at 7 J/cm^2 laser fluence. In this experiment it was also demonstrated that the maximum width of thermal necrosis is $< 85 \mu\text{m}$. The relationship between laser fluence and ablation depth are very similar for both direct laser ablation and fibre delivered laser ablation. This indicates that this fibre based laser scalpel has the capability to excise early stage lesions in the inner lining of the bowel. In conclusion, a promising route towards implementing ps laser surgery in a minimally invasive modality via HC-NCF has been demonstrated.

ACKNOWLEDGMENTS

This research was supported by the UK Engineering and Physical Sciences Research Council (EPSRC) grant reference number EP/N02494X/1. The authors DGJ and NPW are supported by the National Institute for Health Research (NIHR) infrastructure at Leeds. The views expressed are those of the author(s) and not necessarily those of the NHS, the NIHR or the Department of Health. NPW is additionally funded by Yorkshire Cancer Research.

DOI for data set:

10.6084/m9.figshare.7594541

REFERENCES

- [1] J.A. Goldman, J. Chiapella, H. Casey, N. Bass, J. Graham, W. McClatchey, R.V. Dronavalli, R. Brown, W.J. Bennett, S.B. Miller, C.H. Wilson, B. Pearson, C. Haun, L. Persinski, et al., *Lasers Surg Med*, **1980**, 1, 93.
- [2] S.W. Yoo, G. Oh, A.M. Safi, S. Hwang, Y.S. Seo, K.H. Lee, Y.L. Kim, and E. Chung, *Scientific Reports*, **2018**, 8.
- [3] L. Brosseau, V. Welch, G. Wells, P. Tugwell, R. de Bie, A. Gam, K. Harman, B. Shea, and M. Morin, *Journal of Rheumatology*, **2000**, 27, 1961.
- [4] I.M. Varkarakis, T. Inagaki, M.E. Allaf, T.Y. Chan, C.G. Rogers, E.J. Wright, and N.M. Fried, *Urology*, **2005**, 65, 191.
- [5] J.T. Walsh, T.J. Flotte, R.R. Anderson, and T.F. Deutsch, *Lasers in Surgery and Medicine*, **1988**, 8, 108.
- [6] F. Stelzle, I. Terwey, C. Knipfer, W. Adler, K. Tangermann-Gerk, E. Nkenke, and M. Schmidt, *J Transl Med*, **2012**, 10, 123.
- [7] S.X. Li, G. Chen, Y.J. Zhang, Z.Y. Guo, Z.M. Liu, J.F. Xu, X.Q. Li, and L. Lin, *Opt Express*, **2014**, 22, 25895.
- [8] M. Panjehpour, C.E. Julius, M.N. Phan, T. Vo-Dinh, and S. Overholt, *Lasers in Surgery and Medicine*, **2002**, 31, 367.
- [9] O. Dohi, N. Yagi, A. Majima, Y. Horii, T. Kitaichi, Y. Onozawa, K. Suzuki, A. Tomie, R. Kimura-Tsuchiya, T. Tsuji, N. Yamada, N. Bito, T. Okayama, N. Yoshida, et al., *Gastric Cancer*, **2017**, 20, 297.
- [10] J.F. Bille, J.P. Fischer, T. Juhasz, F.H. Loesel, I. MuellerVogt, R. Kessler, S. Goelz, and M.H. Goetz, High precision surface ablation of soft tissue using the fifth harmonic of a Nd:YLF-picosecond laser at 211 nm, *Proceedings Of Lasers in Ophthalmology Iv*, Vienna, Austria, 1996, SPIE, 2930.
- [11] M. Choi and S.H. Yun, *Opt Express*, **2013**, 21, 30842.
- [12] A.A. Oraevsky, L.B. DaSilva, A.M. Rubenchik, M.D. Feit, M.E. Glinsky, M.D. Perry, B.M. Mammini, W. Small, and B.C. Stuart, *Ieee Journal of Selected Topics in Quantum Electronics*, **1996**, 2, 801.
- [13] B. Zysset, J.G. Fujimoto, C.A. Puliafito, R. Birngruber, and T.F. Deutsch, *Lasers Surg Med*, **1989**, 9, 193.
- [14] L.J. Mortensen, C. Alt, R. Turcotte, M. Masek, T.M. Liu, D.C. Cote, C. Xu, G. Intini, and C.P. Lin, *Biomed Opt Express*, **2015**, 6, 32.
- [15] L. Willms, A. Herschel, M.H. Niemz, and T. Pioch, *Lasers in Medical Science*, **1996**, 11, 45.
- [16] H. Huang and Z.X. Guo, *Journal of Physics D-Applied Physics*, **2009**, 42.
- [17] D.F. Hanby, G. Gremillion, A.W. Zieske, B. Loehn, R. Whitworth, T. Wolf, A.C. Kakade, and R.R. Walvekar, *World J Surg Oncol*, **2011**, 9.
- [18] W.H. Noble, K.D. McClatchey, and G.D. Douglass, *J Prosthet Dent*, **1976**, 35, 575.
- [19] J.T. Langell and S.J. Mulvihill, *Med Clin North Am*, **2008**, 92, 599.
- [20] J. Kim, G.J. Lee, J.H. Baek, and W.S. Lee, *Ann Surg Treat Res*, **2014**, 87, 139.
- [21] M.M. Krasnov, *Adv Ophthalmol*, **1977**, 34, 192.
- [22] D. Aronrosa, J.C. Griesemann, and J.J. Aron, *Ophthalmic Surgery and Lasers*, **1981**, 12, 496.
- [23] M. Suguro, T. Hasegawa, S. Suzuki, and F. Hanyu, *Surg Endosc*, **1987**, 1, 131.

- [24] P. Kiefhaber, K. Kiefhaber, and F. Huber, *Endoscopy*, **1986**, 18 Suppl 1, 44.
- [25] T. Schroder, K. Brackett, and S.N. Joffe, *Surgery*, **1987**, 101, 691.
- [26] P. Jaworski, F. Yu, R.M. Carter, J.C. Knight, J.D. Shephard, and D.P. Hand, *Opt Express*, **2015**, 23, 8498.
- [27] P. Jaworski, F. Yu, R.R.J. Maier, W.J. Wadsworth, J.C. Knight, J.D. Shephard, and D.P. Hand, *Opt Express*, **2013**, 21, 22742.
- [28] N.M. Litchinitser, A.K. Abeeluck, C. Headley, and B.J. Eggleton, *Optics Letters*, **2002**, 27, 1592.
- [29] J.D. Shepherd, A. Urich, R.M. Carter, P. Jaworski, R.R.J. Maier, W. Belardi, F. Yu, W.J. Wadsworth, J.C. Knight, and D.P. Hand, *Frontiers in Physics*, **2015**, 3.
- [30] R.J. Beck, W.S. Gora, R.M. Carter, S. Gunadi, D. Jayne, D.P. Hand, and J.D. Shephard, *Precision machining of pig intestine using ultrafast laser pulses*, in *Medical Laser Applications and Laser-Tissue Interactions Vii*. 2015, SPIE: Munich, Germany.
- [31] S.M.P.C. Mohanan, R.J. Beck, W.S. Gora, S.L. Perry, M. Shires, D. Jayne, D.P. Hand, and J.D. Shephard, *Investigation of the efficacy of ultrafast laser in large bowel excision*, *Optical Interactions with Tissue and Cells Xxviii*, Sanfrancisco, USA, 2017, SPIE, 10062.
- [32] D.B. Conkey, E. Kakkava, T. Lanvin, D. Loterie, N. Stasio, E. Morales-Delgado, C. Moser, and D. Psaltis, *Opt Express*, **2017**, 25, 11491.
- [33] E. Kakkava, M. Romito, D.B. Conkey, D. Loterie, K.M. Stankovic, C. Moser, and D. Psaltis, *Biomedical Optics Express*, **2019**, 10, 423.
- [34] K. Gutierrez, N. Dicks, W.G. Glanzner, L.B. Agellon, and V. Bordinon, *Front Genet*, **2015**, 6, 293.
- [35] K. Subramanian, I. Gabay, O. Ferhanoglu, A. Shadfan, M. Pawlowski, Y. Wang, T. Tkaczyk, and A. Ben-Yakar, *Biomed Opt Express*, **2016**, 7, 4639.
- [36] O. Ferhanoglu, M. Yildirim, K. Subramanian, and A. Ben-Yakar, *Biomedical Optics Express*, **2014**, 5, 2023.
- [37] C.R. UK, Bowel cancer mortality statistics
<http://www.cancerresearchuk.org/health-professional/cancer-statistics/statistics-by-cancer-type/bowel-cancer/mortality#heading-Zero>.
- [38] J.H. Hwang, V. Konda, B.K. Abu Dayyeh, S.S. Chauhan, B.K. Enestvedt, L.L. Fujii-Lau, S. Komanduri, J.T. Maple, F.M. Murad, R. Pannala, N.C. Thosani, S. Banerjee, and A.T. Comm, *Gastrointest Endosc*, **2015**, 82, 215.
- [39] A. Vogel and V. Venugopalan, *Chem Rev*, **2003**, 103, 577.
- [40] R.H. Stolen and C. Lin, *Physical Review A*, **1978**, 17, 1448.
- [41] H.P. Weber and W. Hodel, *Physica Scripta*, **1988**, T23, 200.
- [42] R.M. Carter, F. Yu, W.J. Wadsworth, J.D. Shephard, T. Birks, J.C. Knight, and D.P. Hand, *Opt Express*, **2017**, 25, 20612.
- [43] J. Choi and D. Drozek2, *The Open Medical Devices Journal*, **2013**, 5, 1.
- [44] T. Amand and X. Marie, in *Femtosecond Laser Pulses Principles and Experiments*, (Edi.: C. Rulli`ere), Springer Science+Business Media, Inc, USA, 2005. pp. 159.
- [45] J.C. Travers, W.K. Chang, J. Nold, N.Y. Joly, and P.S.J. Russell, *Journal of the Optical Society of America B-Optical Physics*, **2011**, 28, A11.
- [46] M.G. Welch, K. Cook, R.A. Correa, F. Gerome, W.J. Wadsworth, A.V. Gorbach, D.V. Skryabin, and J.C. Knight, *Journal of Lightwave Technology*, **2009**, 27, 1644.
- [47] F. Benabid, J.C. Knight, G. Antonopoulos, and P.S.J. Russell, *Science*, **2002**, 298, 399.
- [48] A. Ben-Yakar and R.L. Byer, *J Appl Phys*, **2004**, 96, 5316.
- [49] W. Kaplonek, K. Nadolny, and G.M. Krolczyk, *Measurement Science Review*, **2016**, 16, 42.

- [50] J.G.R. Bomers, E.B. Cornel, J.J. Futterer, S.F.M. Jenniskens, H.E. Schaafsma, J.O. Barentsz, J.P.M. Sedelaar, C.A. Hulsbergen-van de Kaa, and J.A. Witjes, *World Journal of Urology*, **2017**, 35, 703.
- [51] E. Su, H. Sun, T. Juhasz, and B.J.F. Wong, *Journal of Biomedical Optics*, **2014**, 19.
- [52] A.L. Lazarides, M.J. Whitley, D.B. Strasfeld, D.M. Cardona, J.M. Ferrer, J.L. Mueller, H.L. Fu, S.B. DeWitt, B.E. Brigman, N. Ramanujam, D.G. Kirsch, and W.C. Eward, *Theranostics*, **2016**, 6, 155.
- [53] S.A. Loh, G.A. Carlson, E.I. Chang, E. Huang, D. Palanker, and G.C. Gurtner, *Plastic and Reconstructive Surgery*, **2009**, 124, 1849.
- [54] S. Saha, M. Shaik, G. Johnston, S.K. Saha, L. Berbiglia, M. Hicks, J. Gernand, S. Grewal, M. Arora, and D. Wiese, *Am J Surg*, **2015**, 209, 570.
- [55] S. Sawada, J. Fujisaki, N. Yamamoto, Y. Kato, A. Ishiyama, N. Ueki, T. Hirasawa, Y. Yamamoto, T. Tsuchida, M. Tatewaki, E. Hoshino, M. Igarashi, H. Takahashi, and R. Fujita, *Dig Dis Sci*, **2010**, 55, 1376.